

**MOLYBDENUM VALENCE IN BASALTIC SILICATE MELTS.** L. R. Danielson<sup>1</sup>, K. Righter<sup>2</sup>, M. Newville<sup>3</sup>, S. Sutton<sup>3,4</sup>, K. Pando<sup>1</sup>, <sup>1</sup>Jacobs Sverdrup Co., Houston, TX 77058 United States (lisa.r.danielson@nasa.gov), <sup>2</sup>NASA JSC, 2101 NASA Parkway, Houston, TX 77058 United States, <sup>3</sup>Center for Advanced Radiation Sources and <sup>4</sup>Dept. of Geophys. Sci., University of Chicago, Chicago, IL 60637 United States.

**Introduction:** The moderately siderophile element molybdenum has been used as an indicator in planetary differentiation processes, and is particularly relevant to core formation [for example, 1-6]. However, models that apply experimental data to an equilibrium differentiation scenario infer the oxidation state of molybdenum from solubility data or from multivariable coefficients from metal-silicate partitioning data [1,3,7].

Partitioning behavior of molybdenum, a multivalent element with a transition near the  $fO_2$  of interest for core formation ( $\sim IW-2$ ) will be sensitive to changes in  $fO_2$  of the system and silicate melt structure. In a silicate melt, Mo can occur in either 4+ or 6+ valence state, and  $Mo^{6+}$  can be either octahedrally or tetrahedrally coordinated. Here we present first XANES measurements of Mo valence in basaltic run products at a range of P, T, and  $fO_2$  and further quantify the valence transition of Mo.

Table 1. Experiments analyzed from this and previous studies. Silicate composition is indicated above experiment labels. Piston cylinder experiments [3,5,6] were metal-silicate partitioning studies, while controlled atmosphere experiments had no metal added to the starting composition.

	T deg C	Pressure	$\Delta IW$	Mo, ppm	valence
hawaiite[3]					
66	1300	10 kbar	-0.72	11.78	3.1
83	1300	10 kbar	-0.63	4.61	3.5
basalt[5,6]					
cow1	1500	10 kbar	-1.44	2.9	3.9
cow3	1600	10 kbar	-1.48	4.2	3.9
cow8	1700	10 kbar	-1.45	4.9	4.2
cow20	1800	10 kbar	-1.44	6	3.8
ankaramite					
ankIW	1300	1 bar	0	500	5.3
ankIW1	1300	1 bar	1	500	5.4
ankIW2	1300	1 bar	2	500	6.0
ankIW-1	1300	1 bar	-1	500	3.7
ankIW-2	1300	1 bar	-2	500	2.5
andesite[2]					
KR-D	1190	1 bar	11.5	0.13 wt%	6

**Experiments:** Basaltic run products from 3 previous studies were selected for analyses, with attention to variation in temperature, pressure,  $fO_2$ , and amount of Mo dissolved in the silicate phase (Table 1). A new series of experiments were also conducted at controlled  $fO_2$  in order to more fully explore  $fO_2$  space.

One andesite doped with 0.13 wt%  $MoO_3$  was analyzed from Righter et al. [2], a product that was melted in air. Another set of hawaiites from piston cylinder experiments by Righter and Drake [3] were run at near constant pressure, temperature, and  $fO_2$ , but contain low amounts of Mo from 0.11 ppm to 11.78 ppm by weight. Piston cylinder experiments using a basaltic silicate composition performed by Acuff et al. [5,6] were run at higher temperature and lower  $fO_2$ .

New experiments for this study were performed using ankaramite basalt at conditions similar to the previous study by Danielson et al. [8]. A small amount of Mo dopant (500 ppm) was added to natural ankaramite to ensure detection.

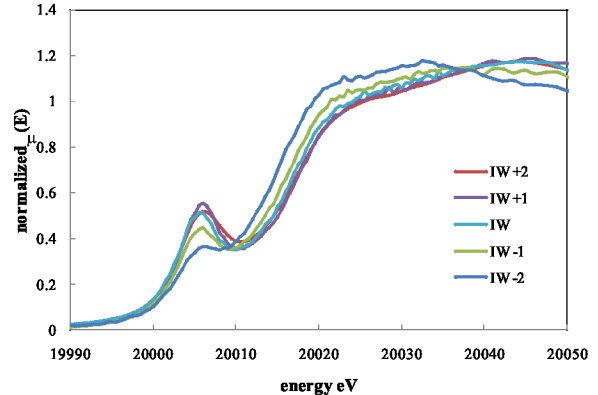


Figure 1. XANES spectra for controlled  $fO_2$  experiments performed for this study, showing K-edge energy shift to lower energy with more reducing conditions. Pre-edge peak (at around 20007 eV) also decreases in intensity. An energy shift of the pre-edge peak to higher eV does not occur, indicating no change in  $Mo^{6+}$  coordination from tetrahedral to octahedral.

**Analyses:** A monochromatic X-ray beam from a Si(111) double crystal monochromator was focused onto the sample and the fluorescent X-ray yield was plotted as a function of incident X-ray energy (more detail can be found in [9]). Mo K XANES spectra were normalized to strontium as an internal reference ele-

ment, then normalized so that the below edge intensity was zero and the above edge intensity was unity. The oxidation state of molybdenum was then inferred from the energy of the K-edge position defined as the lowest energy where  $\mu=1$  in the normalized XANES spectrum (Figure 1) [after 10]. Energy shift and intensity of the pre-edge peak was used to determine coordination of  $\text{Mo}^{6+}$  [10]. Mo foil and experiment KR-D, the extreme oxidized end member Mo doped andesite were used as standards to form a linear trend for valence determination.

**Results and Discussion:** Ankaramite 1 bar experiments show a trend in average valence from  $\text{Mo}^{6+}$  at the most oxidizing condition (IW+2) to nearly  $\text{Mo}^{2+}$  at IW-2 (Figure 2). The transition from  $\text{Mo}^{6+}$  to  $\text{Mo}^{4+}$  occurs largely between IW and IW-1, in good agreement with [7], who concluded Mo changed dominant valence at around IW-1, from  $\text{Mo}^{6+}$  to  $\text{Mo}^{4+}$ . [7] also suggested that below IW, down to IW-3,  $\text{Mo}^{4+}$  and  $\text{Mo}^{6+}$  coexist in equal amounts. Our results narrow the field of  $\text{Mo}^{4+}$  coexistence to IW+1 to just below IW. At the conditions of core formation, near IW-2,  $\text{Mo}^{6+}$  is no longer present. Farges et al. [10] suggested  $\text{Mo}^{5+}$  may be stable around IW. However, [10] evidence for stable  $\text{Mo}^{5+}$  (determined from additional electron paramagnetic resonance spectroscopy data) appears only in FeO-free systems, and thus  $\text{Mo}^{5+}$  is not likely to be present in experiments examined in this study.

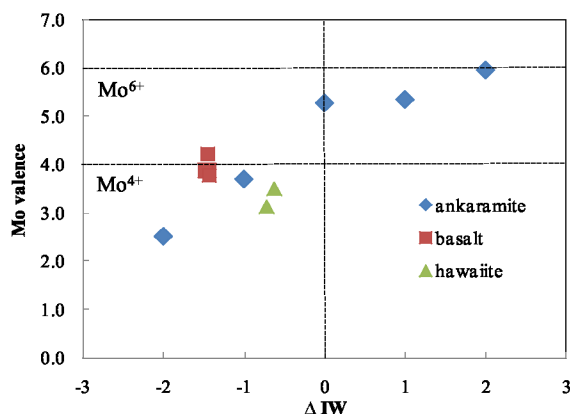


Figure 2. Molybdenum average valence as a function of oxygen fugacity relative to the iron-wüstite buffer for experiments in table 1.

The lack of energy shift of the pre-edge peak (Fig. 1) suggests more than 90% of the  $\text{Mo}^{6+}$  is in tetrahedral coordination. This is the case for all  $f\text{O}_2$  where  $\text{Mo}^{6+}$  is present. Farges et al. [10] supported this system dominated by tetrahedral  $\text{Mo}^{6+}$  - octahedral  $\text{Mo}^{6+}$  only forms where network modifiers become scarce.

As oxygen fugacity decreases below IW-1, contributions from Mo metal increase although Farges et al. [10] maintained that some contributions from  $\text{Mo}^{2+}$  cannot be ruled out. Farges et al. [10] suggested the transition to  $\text{Mo}^0$  dominance happens at around IW-3, with Mo metal becoming visible at IW-4. However, assuming a linear trend in the ankaramite data,  $\text{Mo}^0$  may not be reached until near IW-5. More data will be collected at lower  $f\text{O}_2$  to determine the amount of  $\text{Mo}^0$  contribution.

The moderate increased pressure of the basalt and hawaiiite experiments seems to have no effect on Mo valence, also observed in previous experiments [10]. In silicate melts, but that will be studied in future experiments. In hawaiiites contain up to 1.36% water, this is unlikely to explain any valence differences in experiments around IW-1 [11].

**Conclusions:** Our data support the interpretation of previous authors [1,3,5,6] that  $\text{Mo}^{4+}$  is the dominant species at or below IW-1, with no  $\text{Mo}^{6+}$ , in contrast to the multi-valent Mo in hawaiiites. Conditions below IW-1 may have a significant component of  $\text{Mo}^0$ . Even though the nugget effect has not been reported for Mo at IW-1 or below, a contribution from Mo metal (or even  $\text{Mo}^{2+}$ ) may require modification of metal-silicate partitioning models.

**References:** [1] Holzheid A. et al. (1994) *Geochim. Cosmochim. Acta*, 58, 1975-1981. [2] Righter K. et al. (1998) *Geochim. Cosmochim. Acta*, 62, 2167-2177. [3] Righter K. and Drake M. J. (1999) *Earth Planet. Sci. Lett.*, 171, 383-399. [4] Righter K. (2002) *Icarus*, 158, 1-13. [5] Righter K. et al. (in press) *EPSL*. [6] Acuff K. M. (2008) *LPSC XXXIX*. [7] H. St.C. and Eggins S. M. (2002) *Chem. Geo.*, 186, 151-181. [8] Danielson L. R. et al. (2008) *LPSC XXXIX* 2075. [9] Sutton et al. (2002) *Reviews on Mineralogy & Geochemistry; Appl of Synchrotron Rad in Low-T Geochem & Environ Sci*, Fenter, Rivers, Sturchio, Sutton, eds., *Min. Soc. Amer.*, 429 - 483. [10] Farges F. et al. (2006) *Can. Mineral.*, 44, 731-753. [11] Farges F. et al. (2006) *Can. Mineral.*, 44, 755-773.

**Acknowledgements:** Portions of this work were performed at GeoSoilEnviroCARS (Sector 13), Advanced Photon Source (APS), Argonne National Laboratory. GeoSoilEnviroCARS is supported by the National Science Foundation - Earth Sciences (EAR-0622171) and Department of Energy - Geosciences (DE-FG02-94ER14466). Use of the Advanced Photon Source was supported by the U. S. Department of Energy, Office of Science, Office of Basic Energy Sciences, under Contract No. DE-AC02-06CH11357.